

Predicting Performance using Approximate State Space Model for Liquid State Machines

A. Gorad, V. Saraswat, U. Ganguly

Indian Institute of Technology, Bombay, India, Phone +91 22 2576 7698
ajinkyagorad@ee.iitb.ac.in

Abstract—Liquid State Machine (LSM) is a brain-inspired architecture used for solving problems like speech recognition and time series prediction. LSM comprises of a randomly connected recurrent network of spiking neurons. This network propagates the non-linear neuronal and synaptic dynamics. Maass et al. have argued that the non-linear dynamics of LSMs is essential for its performance as a universal computer. Lyapunov exponent (μ), used to characterize the non-linearity of the network, correlates well with LSM performance. We propose a complementary approach of approximating the LSM dynamics with a linear state space representation. The spike rates from this model are well correlated to the spike rates from LSM. Such equivalence allows the extraction of a memory metric (τ_M) from the state transition matrix. τ_M displays high correlation with performance. Further, high τ_M system require lesser epochs to achieve a given accuracy. Being computationally cheap ($1800\times$ time efficient compared to LSM), the τ_M metric enables exploration of the vast parameter design space. We observe that the performance correlation of the τ_M surpasses the Lyapunov exponent (μ), ($2 - 4\times$ improvement) in the high-performance regime over multiple datasets. In fact, while μ increases monotonically with network activity, the performance reaches a maxima at a specific activity described in literature as the edge of chaos. On the other hand, τ_M remains correlated with LSM performance even as μ increases monotonically. Hence, τ_M captures the useful memory of network activity that enables LSM performance. It also enables rapid design space exploration and fine-tuning of LSM parameters for high performance.

Index Terms—LSM, SNN, State Space model, performance prediction, dynamics, neural networks

I. INTRODUCTION

The brain inspired computational framework of Liquid State Machines (LSMs) was introduced by Maass in 2002 [1]. LSM consist of a large recurrent network of randomly connected spiking neurons called the reservoir. The components of this network, namely the neurons and synapses, all follow highly non-linear dynamics. Depending on the extent and strength of connectivity, the reservoir propagates this non-linear dynamics in a recurrent manner. Maass et al. have argued that these non-linear operations performed by LSMs allow it to display high performance and universal computational capabilities [1]. Many applications are based on the belief that non linearity of the LSMs enable powerful data processing [2]–[4]. In [3] non-linear computations were performed on time series data. In [4], LSM was used for movement prediction task and was shown to perform a non-linear technique of Kernel Principal Component Analysis. Speech recognition, time series prediction, and robot control are few of the many versatile applications for which LSM has demonstrated excellent performance [2], [5]–[7].

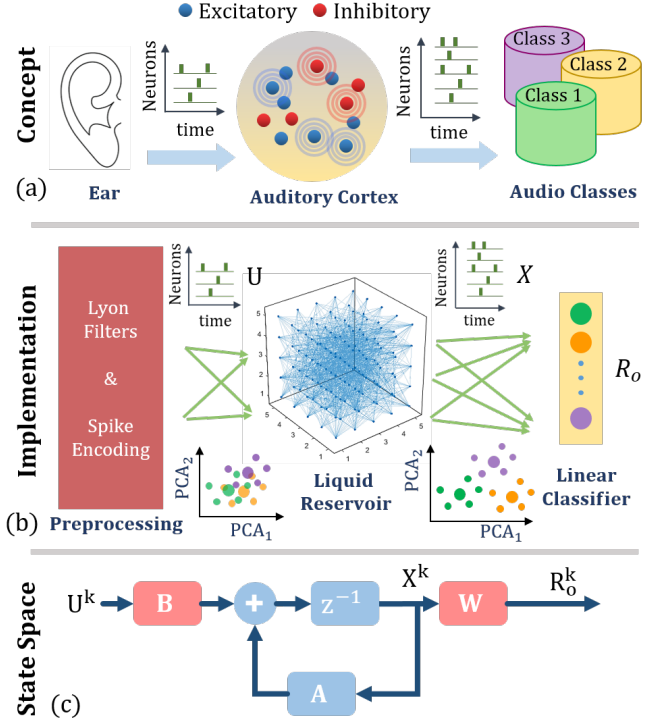


Fig. 1. Architecture of Liquid State Machine (LSM) showing an example for speech recognition. (a) Conceptual description: Spikes generated in the cochlea (ear) travel to the auditory cortex where a randomly connected recurrent neural network acts as a reservoir of a liquid where input spikes produce a "ripple-like" memory in the network. The output of the network transform the non-linearly separable input in low dimensions to a linearly separable output in a higher dimension to enable a simple classifier to perform accurate classification. (b) Implementation of the LSM concept in MATLAB consists of a pre-processing layer (using Lyon's Filter) to generate a spike input, a liquid reservoir of randomly connected recurrent spiking neurons and a linear readout classifier. (c) Discrete Linear State Space approximation of LSM with input mapping B , state transition matrix A and readout weight matrix W .

LSMs have a vast set of design parameters with no direct relation with the performance. It is also known that, depending on the reservoir connectivity, an LSM may function in the region of low propagation i.e. input spikes may cause a chain reaction in neurons in the LSM to propagate spikes in the network for a short time. Higher propagation may ultimately lead to chaotic dynamics [8]. However, in order to achieve the best performance, the network has to function at an optimal level of activity or, as the literature cites it, at the "edge of

chaos” [9]. Many attempts have been made to define metrics to capture the network dynamics that correlates with this trend in performance of LSMs [8], [10]–[13]. Inspired by the idea to capture the extent of non-linear dynamics in the network, Lyapunov exponent is the most successful metric which is well-correlated with the LSM’s performance [10]. Simply put, Lyapunov exponent characterizes the network by measuring the difference in output for two almost identical inputs as the measure of the network’s ability to resolve small differences in inputs. As such, it is not an equivalent model for LSM.

State space is an established mathematical modelling framework especially for time-evolution in linear systems. The framework has a rich legacy of intuition and rigorous techniques for stability analysis, feedback design for controllers - the many utilities that state space modelling has to offer [14].

In this work, we model the LSM as a linear state space model. We demonstrate that the spike rates obtained from the linear state space representation are well correlated with the spike rates from the exact simulations of LSM. The level of similarity or correlation of the linear model with the exact dynamics depends on the region of performance the LSM is operating in. An LSM operating in the region of high accuracy is indeed well modelled by the linear state space. We show that key advantage of a first order model is that it allows us to evaluate a “memory” metric τ_M for the system which shows high correlation with the network performance. τ_M provides a computationally cheap approach to exploring the design space of the LSMs which have a vast number of design parameters. In addition, we find that the new proposed metric τ_M surpasses the performance prediction capabilities of the Lyapunov exponent. τ_M is able to capture the optimal performance achieved as a function of the network activity believed to be occurring at the “edge of chaos” [9]. For fine tuning performance of LSMs, τ_M is shown to be better than Lyapunov exponent over multiple datasets.

The paper is organized as follows: Section II highlights how LSMs have been implemented to achieve accuracy comparable to the state-of-the-art for the TI-46 speech dataset. In Section III, the state space model is presented to calculate the linear approximation of the LSM behavior and extract the memory metric. Section IV consists of the results and discussions, where τ_M is calculated for LSMs exhibiting a range of performances. We show that τ_M significantly outperforms Lyapunov exponent for high performance LSMs.

II. BACKGROUND

Liquid State Machine (LSM) framework [1] is analogous to the brain, where, for e.g. external sensory stimuli like sound is converted to spikes through cochlea in ear. These spikes go to the auditory cortex which form ripples of network activity to enable the conversion of a linearly inseparable input at lower dimensions to a linearly separable output at higher dimensions which are easy to classify (Fig. 1 (a)). The implementation of LSM architecture consists of (i) a pre-processing layer where sound is converted to spike trains. (ii) These spikes are introduced to the randomly connected spiking neural network

called liquid or reservoir. Here input spikes produce a wave of spikes in the randomly connected recurrent spiking neural network which is similar to a liquid where raindrops cause ripples to propagate (carrying the memory of the raindrops) and eventually fading away. Thus, a network of fixed synaptic weights and delays in the reservoir spreads the input across time and space (i.e. among neurons). The small number of inputs are translated by the large network on neurons in the LSM to a higher dimensions. This higher dimensional liquid response improves the performance of a simple classifier layer with a learning rule.

A. Speech preprocessing

Speech pre-processing stage for an LSM consists of a human ear-like model, namely Lyon’s Auditory Cochlear model [21]. It consists of a cascade of second order filters to produce a response for each channel. The output of each second order filter is rectified and low-pass filtered to get smooth signal. The shape of the second order filters is determined by the quality factor Q and its step size Δ_{step} [19]. Human ears have a large dynamic range (60-80 dB), thus, an Automatic Gain Control (AGC) stage with particular target amplitude A_m and timescale τ_{AGC} is incorporated in the Lyon’s model. Since the samples in TI-46 dataset have the sampling rate of 12.5 KHz, the output of this AGC, called cochleogram was decimated in time by decimation factor df of 12 for simulation purposes. This was done with the help of Auditory Toolbox in MATLAB [19]. This decimated output is converted into spikes trains using BSA algorithm [20]. A second order filter h_{BSA} was used for this encoding scheme with the time constants of τ_{b1} & τ_{b2} . Finally, 77 spike trains were generated for a corresponding input speech sample in the preprocessing stage. Relevant parameters for this stage are given in Table I.

$$h_{BSA} = (e^{-\frac{t}{\tau_{b1}}} - e^{-\frac{t}{\tau_{b2}}})H(t) \quad (1)$$

TABLE I
PREPROCESSING PARAMETERS

Parameter	Value	Parameter	Value
Q	8	df	12
Δ_{step}	0.25	τ_{b1}, τ_{b2}	4, 1 ms
A_m	0.0004	τ_{AGC}	32 ms

B. Liquid Reservoir

Liquid Reservoir is taken to be a 5x5x5 3D grid of Leaky Integrate and Fire (LIF) neurons with fraction f_+ as excitatory and the rest as inhibitory neurons in the simulations. Neural dynamics are given by (2)-(3), where V is the membrane potential with time constant τ_{Neu} , refractory period T_{rp} , threshold voltage V_{th} and elicited spike time t_s , v is the synaptic input to the neuron. w_{ij} is the connection strength from N_i to N_j .

$$\frac{\partial V}{\partial t} = -\frac{V}{\tau_{Neu}} + \sum_i \sum_j w_{ij} v_j \quad (2)$$

$$V > V_{th} \rightarrow V = 0 \quad \forall \quad t_s < t < t_s + T_{rp} \quad (3)$$

TABLE II
DEFAULT NETWORK PARAMETERS

Parameter	Value	Parameter	Value	Parameter	Value
W_{EE}	3	K_{EE}	0.45	τ_{1E}	8 ms
W_{EI}	6	K_{EI}	0.3	τ_{2E}	4 ms
W_{IE}	-2	K_{IE}	0.6	τ_{1I}	4 ms
W_{II}	-2	K_{II}	0.15	τ_{2I}	2 ms
W_{in}	± 8	f_+	0.85	λ	2
F_{in}	4	d_{ij}	1 ms		

Neurons are connected with synapses of specific weights by the probabilistic rule given in (4), where $D(N_1, N_2)$ is the distance between neurons N_1 and N_2 in the reservoir, λ is the effective synaptic distance. K is the connection probability, and it can take values as K_{EE} , K_{EI} , K_{IE} , K_{II} . For e.g. K_{EI} corresponds to the probability of connection from excitatory (E) to inhibitory (I) neuron along with the radial dependence (4).

$$P(N_1, N_2) = K \cdot e^{-\frac{D^2(N_1, N_2)}{\lambda^2}} \quad (4)$$

Similarly, synaptic weights w_{ij} can take values W_{EE} , W_{EI} , W_{IE} , W_{II} in the liquid (where subscripts denote E: Excitatory, and I: Inhibitory e.g. W_{IE} denotes weight of the inhibitory to excitatory connection) and are constant in time. Synaptic delays are fixed to d_{ij} for every synapse. Both the excitatory and inhibitory synapses are second order and follow the timescales of (τ_{1E}, τ_{2E}) for excitatory and (τ_{1I}, τ_{2I}) for inhibitory connections in the reservoir. These timescales correspond to τ_1 and τ_2 for synaptic dynamics given by (5), where H is the unit step function.

$$v = \frac{1}{\tau_1 - \tau_2} (e^{-\frac{t-t_s}{\tau_1}} - e^{-\frac{t-t_s}{\tau_2}}) H(t - t_s) \quad (5)$$

Each input spike train from the preprocessing stage is given to randomly chosen F_{in} neurons in the reservoir with uniformly distributed synaptic weights of $\pm W_{in}$. For these synapses, only excitatory timescales were used. Default network parameters for simulations on TI-46 dataset are given in Table. II, which are also mentioned in [15].

C. Classifier

To recognize the class of the input from the multidimensional liquid response, generally, a fully connected layer of spiking readout neurons is used. Excitatory timescales were used for both excitatory and inhibitory synapses connecting the reservoir to the classifier. Since the only weight update in an LSM are to happen here, it needs a learning rule which learns the weights to extract useful features from the reservoir. After training, the class corresponding to the most spiked neuron is regarded as the classification decision of the LSM for the given input.

We briefly describe the biologically inspired learning rule proposed in [15]. It uses calcium concentration, c for depicting the activity of the neuron in the classifier to enable selective weight change during a training phase. The calcium

concentration for a neuron is defined by a first order equation (6) with timescale τ_c . Steady state concentration c_s is approximately given by (7) and is the indicator of spike rate (f_r) of the neuron. Supervised learning with large forcing current I_{teach} is used depending on the activity and desirability (or undesirability) of the neuron. The desired (or undesired) neuron is supplied I_∞ (or $-I_\infty$) current to spike more (or less) for the present training input. For each output neuron, this rule uses a probabilistic weight update according to (9), (10) for the corresponding synapse whenever pre-neuron in the reservoir spikes. A constant weight update Δw is added or subtracted, with probability p^+ or p^- respectively, to the present synaptic weight depending on the input class and the limit on the activity (decided by c_θ & Δc). Hence, the weight is increased/decreased if the pre-neuron spikes and the classifier neuron is the desired/undesired neuron (9), (10). This weight is artificially limited by value W_{lim} . The default parameters are mentioned in Table. III.

$$\frac{\partial c}{\partial t} = -\frac{c}{\tau_c} + \delta(t - t_s) \quad (6)$$

$$c_s = \frac{1}{e^{\frac{T_s}{\tau_c}} - 1} \approx \tau_c f_r \quad (7)$$

$$I_{teach} = \begin{cases} +I_\infty \cdot H((c_\theta + \delta c) - c), & \text{if desired} \\ -I_\infty \cdot H(c - (c_\theta - \delta c)), & \text{if undesired} \end{cases} \quad (8)$$

$$w \xrightarrow{p^+} w + \Delta w; \quad c_\theta < c < c_\theta + \Delta c \quad (9)$$

$$w \xrightarrow{p^-} w - \Delta w; \quad c_\theta - \Delta c < c < c_\theta \quad (10)$$

TABLE III
NEURON & CLASSIFIER PARAMETERS

Parameter	Value	Parameter	Value	Parameter	Value
τ_{Neu}^*	64 ms	c_θ	10	W_{lim}	8
T_{rp}	3 ms	Δc	2	p^\pm	0.1
V_{th}	20 mV	δc	1	Δw	0.01
I_∞	10000	τ_C	64 ms		

D. Performance

We replicated the setup from [15], and matched the state-of-the-art performance for the chosen reservoir size of 5x5x5 for TI46 speech dataset (Table. IV). System is trained and for 200 epochs on 500 TI-46 spoken digit samples. Performance is evaluated using 5 fold testing where accuracy is averaged over the last 20 epochs [15]. Samples used in training and testing consisted of a uniform distribution of 50 samples for each digit ‘0-9’ and 100 samples for each speaker, among 5 female speakers. Time step of 1ms was used in all the simulations. Simulation was done in Matlab and took a wall-clock time of 14 hours for each run on a Intel Xeon processor running at 2.4 GHz.

E. Reservoir-less Network

We use a feed-forward fully-connected reservoir-less network to benchmark against the LSM. We train the same

TABLE IV
LSM PERFORMANCE ON SPOKEN DIGIT RECOGNITION

Work	Dataset	Accuracy (%)
Our	TI-46	99.09
Zhang et al. [15]	TI-46	99.10
Verstraeten et al. [2]	TI-46	99.5
Wade et al. [24]	TI-46	95.25
Dibazar et al. [23]	TIDigits	85.5
Tavanaei et al. [22]	Aurora	91

preprocessed input on the same classifier. The difference between the performance by this method and the performance by the LSM is the gain/loss in the performance by introducing the reservoir. Generally, LSMs will benefit from the higher dimensional mapping and the recurrent dynamics of the network.

III. METHODOLOGY

This section describes how the discrete state space approximation was developed for the LSM dynamics described in the background and the resulting memory metric.

A. State Space Approximation

To study the dynamics of the spiking trajectories of LSM, we consider the spike rate column vectors for input (U^k), reservoir (X^k) and readout (R_o^k), where each row of the vector corresponds to a instantaneous spike rate at time k for a neuron. Spike rate activity calculated as the average number of spikes in a rectangular window of 50 ms, and is a column vector where each row corresponds to a neuron. This spike rate activity spans a trajectory in a multi-dimensional space (each dimension is represents a different neurons) with time [18].

The input activity U^k gets mapped to the higher dimensional space of the reservoir. The future activity or state of the liquid X^{k+1} can be written as a function f of its present input U^k and the current state X^k (11). Also, since the readout function does not possess any memory, it can be simply the function f_w of reservoir activity X^k (12).

$$X^{k+1} = f(X^k, U^k) \quad (11)$$

$$R_o^k = f_w(X^k) \quad (12)$$

Dynamics of the LSM are approximated using a state space model which is first order and linear (Fig. 1 (c)). Reservoir (11) and the readout (12) are approximated by (13) and (14) respectively using constant matrices A , B and W .

$$X^{k+1} = A \cdot X^k + B \cdot U^k \quad (13)$$

$$R_o^k = W \cdot X^k \quad (14)$$

Let U , X and R_o be the actual LSM simulated spike rate over time of all the 10 samples after the training. We denote shifted version of matrix X by 1 time step in future as X_{+1} . We estimate A, B and W by taking the Moore-Penrose inverse ($pinv$) of the combined matrix of X and U of the system by knowing the spike rate of input, reservoir and readout neurons on chosen 10 samples (16), (17). For a system with M input,

N reservoir and L readout neurons, we get size of A to be $N \times N$, B to be $N \times M$ and W to be $L \times N$. Concatenation of matrices X and U is represented as $[X|U]$.

$$X_{+1} = [A|B] \cdot [X|U]^T \quad (15)$$

$$\Rightarrow [A|B] = X_{+1} \cdot pinv([X|U]^T) \quad (16)$$

$$R_o = W \cdot X \Rightarrow [A|B] = R_o \cdot pinv(X) \quad (17)$$

Once A , B and W are determined, Knowing only the input U , we estimate the \hat{X} and, finally, \hat{R}_o from the estimated \hat{X} . To evaluate the effectiveness of state space modelling of an LSM, we find the correlation coefficient of the actual response X with predicted response \hat{X} knowing the input ($U \rightarrow \hat{X}$). We also evaluate other combinations of prediction to see how well this approximation holds. Forward combinations include $U \rightarrow \hat{X}$, $X \rightarrow \hat{R}_o$ and $U \rightarrow \hat{X} \rightarrow \hat{R}_o$. Reverse combinations include $R_o \rightarrow \hat{X}$, $X \rightarrow \hat{U}$ and $R_o \rightarrow \hat{X} \rightarrow \hat{U}$. This correlation coefficient qualifies the ability of state space to model LSM (discussed in Section IV).

B. Concept of memory

For an N dimensional state space represented by X given by (18) having N time constants τ_i . Memory of such a system can be defined as the mean of the time constants τ_i (19).

$$\dot{X} = -diag(\frac{1}{\tau_1}, \frac{1}{\tau_2}, \dots, \frac{1}{\tau_N}) \cdot X \quad (18)$$

$$\tau_M = \frac{1}{N} \sum_{i=1}^N \tau_i \quad (19)$$

A discrete first order system with time constant τ_i is represented as (20) using Euler method. Here, h is the time step of the discretized system.

$$x_i^{k+1} = (1 - \frac{h}{\tau_i})x_i^k \quad (20)$$

For a system matrix A of size $N \times N$ in a discrete state space system which defines the time dynamics, we get its diagonal entries in vector a . From this, we propose the memory metric τ_M for an approximate model of the reservoir (13) to be (22). In our case, discrete time step h is 1ms.

$$a = diag(A) \quad (21)$$

$$\tau_M = \frac{1}{N} \sum_{i=1}^N \frac{h}{1 - |a_i|} \quad (22)$$

This memory metric is calculated and its relation with performance is explored (presented in Section IV). It is also compared to the previously identified state of the art performance prediction metric Lyapunov exponent (μ) [10]. Intuitively, Lyapunov exponent simply characterizes the chaotic behaviour of the network by measuring the difference in output for two almost identical inputs as the measure of the network's ability to resolve small differences in inputs. As such, it is not an equivalent model for LSM. It is calculated

as the average over the scaled exponents (μ_i) for classes $i = 1, 2, \dots, 10$, where for each class i , μ_i is calculated from two samples u_{1i} , u_{2i} and their reservoir response x_{1i} , x_{2i} using (23).

$$\mu_i = \ln \frac{\|x_{1i}(t) - x_{2i}(t)\|}{\|u_{1i}(t) - u_{2i}(t)\|} \quad (23)$$

C. Simulation Methodology

The reservoir in an LSM has a large number of parameters defining its design space. Study by [17] identified few key parameters, which include synaptic scaling α_w and effective connectivity distance λ . We vary the given synaptic weights by a constant factor α_w . We simulate the LSM for speech recognition task using TI-46 dataset and evaluate the performance over 12 different α_w , each comprising of 4 randomly generated structures for the same parameter settings.

IV. RESULTS AND DISCUSSION

A. Similarity to State Space

We estimate the reservoir spikes \hat{X} and find them to be well matched with the actual spike rate X for the transformation $U \rightarrow \hat{X}$ using the state space approximation with Pearson Correlation Coefficient (PCC) of 0.92. Figure 2 shows the visual representation of actual reservoir spike rate and the estimated spike rate for each neuron in the reservoir in the high performance region of operation.

Further, correlation coefficients for all model estimated spike rates with exact spike rates are evaluated as a function of performance for both the forward and reverse pathways (Fig. 3). Forward estimation gave higher correlation values than reverse estimation. Further, when estimating the reservoir spikes from the input spikes ($U \rightarrow \hat{X}$), we find that this model is a good fit when error is small. In other words, the mapping of LSM to state space is more accurate when the output performance of the network is high.

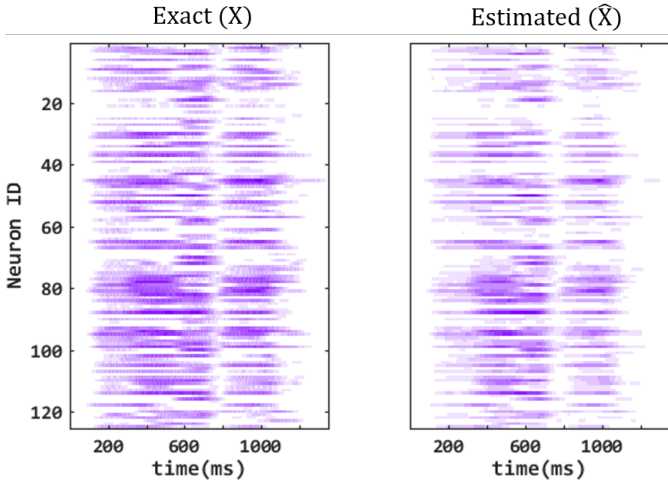


Fig. 2. Well correlated (Pearson Correlation Coefficient i.e. PCC = 0.92) reservoir spike rates for LSM X and state space estimation \hat{X} for each neuron in the reservoir as a function of time for a speech sample from TI-46 dataset.

We obtain the state space model estimation of the readout f_w by W with correlation greater than 0.85 for all ranges of error ($X \rightarrow \hat{R}_o$). The overall transition from $U \rightarrow \hat{X} \rightarrow \hat{R}_o$ is the combination of $U \rightarrow \hat{X}$ & $X \rightarrow \hat{R}_o$ and hence, the correlation between R_o and \hat{R}_o given the input U is lower than both.

The mapping from readout to reservoir ($R_o \rightarrow \hat{X}$) gives weak correlation coefficients in reverse estimation. This is intuitively expected as the readout need not represent all the information in the liquid mainly because the classifier has a lower dimensionality of 10 compared to 125 in the reservoir. In comparison, when we estimate the input (of dimensionality 77 in these simulations) from the reservoir $X \rightarrow \hat{U}$, the correlation is close to 0.8, and overall estimation correlation $R_o \rightarrow \hat{X} \rightarrow \hat{U}$ is less than both $R_o \rightarrow \hat{X}$ & $X \rightarrow \hat{U}$.

B. Performance as a function of Network Activity

We calculate the performance and the memory metric in different regimes of the LSM operation. For different reservoir weight scaling α_w (also called synaptic weight scaling) we obtain low-propagation (sparse activity $\alpha_w = 0.5$), significant-propagation (normal activity $\alpha_w = 0.8$), in-chaos (high activity $\alpha_w = 2$) and saturation (all neurons spiking $\alpha_w = 5$), shown in Fig.4 (a). Performance of the LSM for various synaptic weight scaling is found (Fig. 4 (b)) and the memory metric τ_M of the corresponding state space modelled system is found using (22), and its variation against synaptic weight scaling is shown in Fig. 4 (c).

For low-propagation in the reservoir where α_w is 0.5, there is mainly higher dimensional mapping of the input and limited dynamics take place in the reservoir. This higher dimensional mapping gives a boost of 5% to the accuracy 93% of reservoir-

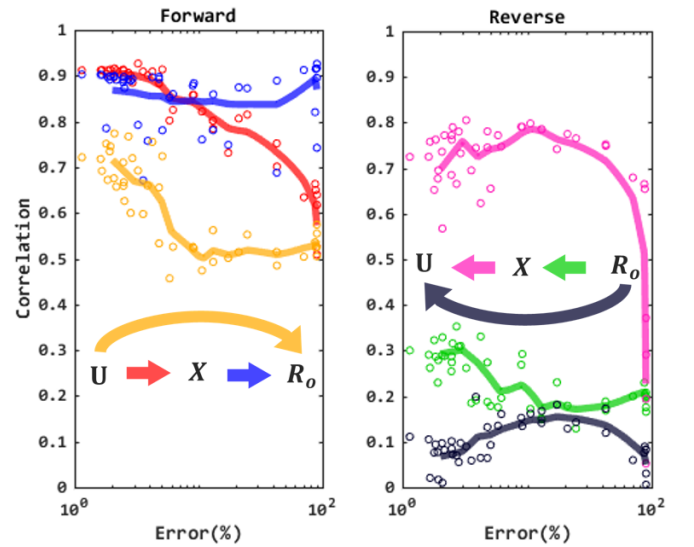


Fig. 3. Average correlation coefficient between LSM and State Space Model spike rates vs. error (log scale) for all the possible transformations on all 500 samples of TI-46 dataset. Forward correlation are stronger than backward correlations. In the forward transformations, correlations improve in low error (high accuracy) regime.

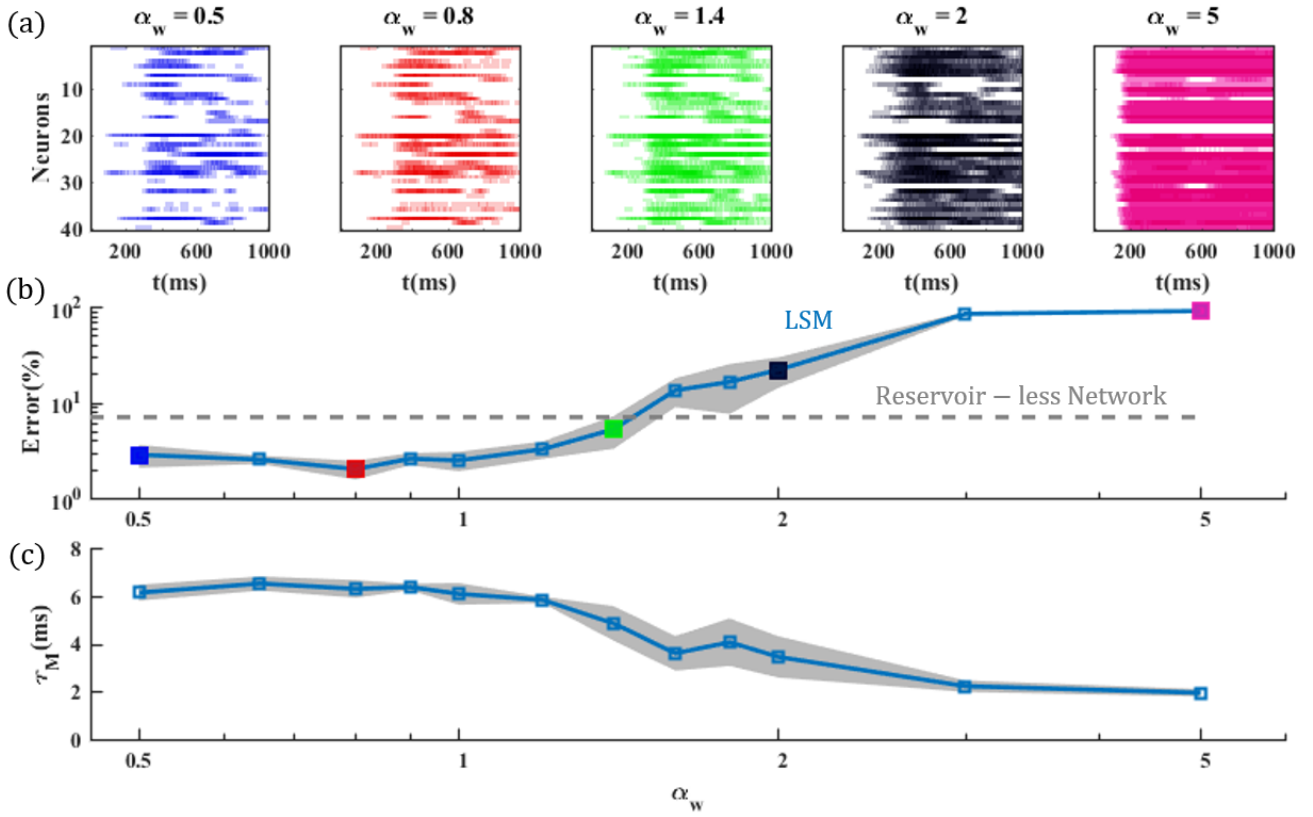


Fig. 4. (a) Spike rate in the reservoir vs. synaptic scaling (α_w) for 40 neurons resulting from a TI-46 speech sample. At the optimal value of $\alpha_w = 0.8$, the spike propagation is optimal which related to high accuracy. At lower α_w (< 0.8), the spike propagation is weak and reduces accuracy. For higher α_w (> 0.8), the spike propagation is excessive, leading to degraded performance. Higher $\alpha_w = 5$, leads to relentless spiking. (b) Error vs. synaptic weight scaling and (c) Memory metric τ_M vs. synaptic scaling both show non-monotonic but correlated dependence. One sigma variation over different runs is also plotted in grey in (b) and (c). The performance of a reservoir-less network, where the input is directly connected to the classifier, is shown in comparison to an LSM.

less approach (Fig. 4). Increasing the weights ($\alpha_w = 0.8$) allows input spikes to propagate through the reservoir and hence allows memory dynamics, which contribute to the performance. This results in the reduction of error to 1.5%. The size of the LSM and activity together maximize the accuracy which corresponds to increase in the memory metric.

However, increasing activity does not always correspond to good performance, and hence should also not contribute to the memory of useful information present in the system. Our proposed memory metric decreases because of the increasing activity, as the disorder increases and the LSM enters chaos. In saturation regime ($\alpha_w = 5$), it is evident that there is not much useful information as the pattern is lost permanently.

We think that the state space approach helps in characterizing the memory of LSM, because, useful information is related in time by its past activity and the current input. This approximation of trajectories provides an estimate of how the system evolves with the addition of new input. As the LSM enters chaotic regimes, the information is actually destroyed due to disturbance of this trajectory, this is highlighted by the breaks in the trajectory and cannot be captured by the smooth state space transition.

C. Comparison with Lyapunov Exponent

Following from the above discussion, the key property of the proposed memory (τ_M) metric that emerged on varying the synaptic weight scaling (α_w) is that τ_M has very high correlation with the recognition performance, i.e. large memory results in higher accuracy (Fig. 5 (a)). A more significant trend is observed when we focus on the high performance region. The PCC of τ_M with accuracy was found to be 0.93 over all possible error values and it increased to 0.95 for points in close proximity to small error (Fig. 5 (b)). As a comparison benchmark, we also calculated the absolute PCC with accuracy of the previously identified [10] state-of-the-art performance prediction metric, Lyapunov exponent (μ) as 0.95 which rapidly dropped down as we focused on the high performance region of operation (Fig. 5 (b)). In other words, the overall performance correlation for both the metrics is at par, however, τ_M performs better than μ for low error regions. This is due to the monotonic nature of Lyapunov exponent with respect to synaptic scaling. In general the accuracy of LSMs increase as the activity increases but then reduces with the onset of chaos. τ_M captures this optimal activity threshold precisely increasing its utility over the Lyapunov exponent.

In addition, this behavior of τ_M is general and can be

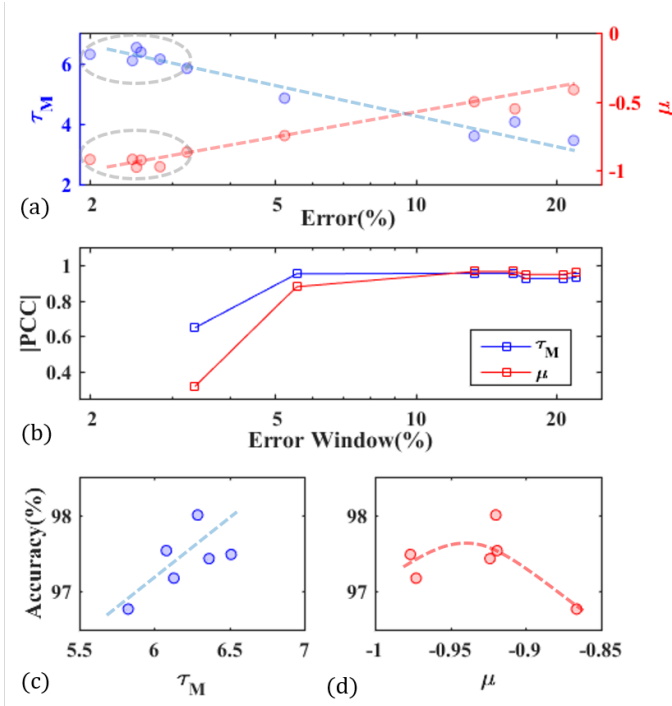


Fig. 5. (a) Correlation of τ_M and μ with error for TI-46 speech dataset. (b) For overall error range, the correlation values are comparable for τ_M and μ (0.96). Correlation of τ_M (0.64) with accuracy is $2\times$ higher than that of μ (0.31) at lower errors is also seen by the low error expanded view behaviors in (c) and (d) of the encircled regions in (a)

extended to other datasets. We adopt a well known strategy for generating another test dataset [17], [25]. We construct 10 input spike train templates of 40 Hz poisson distributed, each comprising 10 spike channels with sample length of 200 ms. From each of them we generate 50 spike patterns, where spike of each template is jittered temporally with standard deviation of 16 ms. Any resulting spikes outside the window of sample are removed. We train this dataset for 100 epochs on the LSM with a different set of reservoir parameters as mentioned in [17] and vary the synaptic scaling from 0.1 to

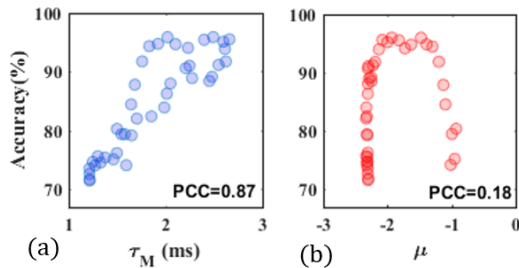


Fig. 6. Performance dependency with our memory metric τ_M and Lyapunov exponent μ for generated poisson spike dataset. Synaptic weight scaling α_w was varied. Values are shown for average accuracy over last 20 epochs from total of 100 epochs for 2-fold testing. Significantly better correlation ($> 4\times$) to performance is observed in case of τ_M (0.87) compared to Lyapunov exponent (0.18) for the network.

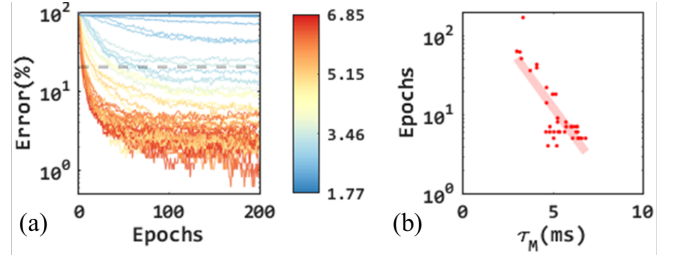


Fig. 7. (a) Error vs epochs with its memory metric τ_M (ms) (color) for TI-46 dataset. Dashed grey line indicates error at which points are plotted in (b). (b) Number of epochs required for achieving 80% accuracy. Lower epochs are required to achieve same accuracy for higher τ_M

4. With this dataset, we found the PCC of memory metric to the performance to be 0.87 (Fig. 6 (a)), which is significantly greater than PCC of 0.18 (Fig. 6 (b)) for the Lyapunov exponent. This suggests memory metric τ_M is a better measure for performance with increased generality across datasets.

Another attractive property of τ_M is the associated time efficiency of the system to achieve a given accuracy. Fig. 7 (a) shows a large density of high τ_M systems achieving greater accuracy more quickly (in lower number of epochs). For performance to fall below a specified error, we get an exponential relationship between the number of epochs required and the associated memory metric of the system (Fig. 7 (b)). In other words, the memory metric has a direct impact on the learning rate of the classifier with faster learning being enabled in high τ_M systems.

D. Computational Efficiency

One simulation of exact LSM takes 1.5 hrs on average, if the system is trained for only 20 epochs. In comparison, one τ_M extraction from the approximate state space modelling takes only 3 seconds which is an $1800\times$ speed up. Further, τ_M calculation is $2\times$ faster than the calculation for the Lyapunov exponent.

E. Design Space Search

Given the performance predictive properties of τ_M , the design space exploration is greatly simplified for LSMs. As highlighted in the simulation methodology, LSMs can be tuned by varying a large number of parameters. To highlight the utility of τ_M in this regard, we use previously identified synaptic scaling (α_w) and effective connectivity λ as the key performance parameters [17] to explore the accuracy achieved. We compare the accuracy with the calculated τ_M and μ over the same parameter space. The accuracy shows a region of maxima (dark green - Fig. 8 (a)) and falls off on either side over the parameter space. This behavior can also be seen for the τ_M obtained over the same parameter space (Fig. 8 (b)). Hence, calculation of τ_M from state space approximation provides an efficient method to identify the correct parameter values for high performing LSM. Again, as discussed earlier in Fig. 5, the Lyapunov exponent does not capture the performance optima unlike τ_M and is monotonic in

nature with network activity. Correlation was found to be 0.90 for the memory metric and 0.18 for the Lyapunov exponent in the high performance region (Accuracy > 85%) for the design space search conducted over α_w and λ (Fig. 8).

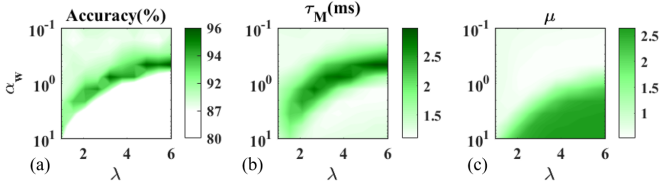


Fig. 8. The memory metric is used for design space search using Poisson Spikes dataset, where space is explored over reservoir synaptic scaling α_w and effective connectivity λ . On the grid of 10×10 , shown are the (a) LSM simulation result with average accuracy over last 5 epochs from total 20 epochs with 2-fold testing (b) Our memory metric τ_M (c) Lyapunov exponent μ . We observe that high performance regions are clearly highlighted by the memory metric, while Lyapunov exponent does not captures the optimal space of α_w and λ as it shows a monotonic trend. Higher PCC (5x) with performance was observed for τ_M (0.90) compared to μ (0.18).

V. CONCLUSION & FUTURE WORK

It is widely believed that recurrent network of non-linear elements producing highly non-linear information processing to enable high performance in recognition tasks. In this paper, we present an alternative interpretation of LSM where we approximate it with a linear state space model - a well-established mathematical framework. We demonstrate high correlation of the model response with the LSM. Equivalence with state space allows the definition of a memory metric which accounts for the additional performance enhancement in LSMs over and above the higher dimensional mapping. The utility of τ_M as a performance predictor is general across datasets and is also responsible for time efficient learning capabilities of the classifier at the output. We compare and highlight the advantages of τ_M over the existing state-of-the-art performance predictor metric Lyapunov exponent μ , where a 2-4 \times improved correlation of accuracy is observed for τ_M . τ_M captures the maximum performance for optimum parameters in the design space where the network has optimal activity is at the “edge of the chaos”. In contrast, Lyapunov exponent is monotonic with network activity - resulting in poor performance prediction at high performance. Further, the computational efficiency of the state space model (1800 \times compared to LSM) to compute τ_M enables rapid design space exploration and parameter tuning.

REFERENCES

- [1] Maass, W., Natschlger, T., & Markram, H. (2002). Real-time computing without stable states: A new framework for neural computation based on perturbations. *Neural computation*, 14(11), 2531-2560.
- [2] Verstraeten, D., Schrauwen, B., Stroobandt, D., & Van Campenhout, J. (2005). Isolated word recognition with the liquid state machine: a case study. *Information Processing Letters*, 95(6), 521-528.
- [3] Maass, W., Natschlger, T., & Markram, H. (2004). Computational models for generic cortical microcircuits. *Computational neuroscience: A comprehensive approach*, 18, 575.
- [4] Burgsteiner, H., Krill, M., Leopold, A., & Steinbauer, G. (2007). Movement prediction from real-world images using a liquid state machine. *Applied Intelligence*, 26(2), 99-109.

- [5] Rossell, J. L., Alomar, M. L., Morro, A., Oliver, A., & Canals, V. (2016). High-density liquid-state machine circuitry for time-series forecasting. *International journal of neural systems*, 26(05), 1550036.
- [6] de Azambuja, R., Klein, F. B., Adams, S. V., Stoelen, M. F., & Cangelosi, A. (2017, May). Short-term plasticity in a liquid state machine biomimetic robot arm controller. In *2017 International Joint Conference on Neural Networks (IJCNN)* (pp. 3399-3408). IEEE.
- [7] Das, A., Pradhapan, P., Groenendaal, W., Adiraju, P., Rajan, R. T., Catthoor, F., ... & Van Hoof, C. (2018). Unsupervised heart-rate estimation in wearables with Liquid states and a probabilistic readout. *Neural Networks*, 99, 134-147.
- [8] Schrauwen, B., Bsing, L., & Legenstein, R. A. (2009). On computational power and the order-chaos phase transition in reservoir computing. In *Advances in Neural Information Processing Systems* (pp. 1425-1432).
- [9] Legenstein, R., & Maass, W. (2007). What makes a dynamical system computationally powerful. *New directions in statistical signal processing: From systems to brain*, 127-154.
- [10] Chrol-Cannon, J., & Jin, Y. (2014). On the correlation between reservoir metrics and performance for time series classification under the influence of synaptic plasticity. *PloS one*, 9(7), e101792.
- [11] Goodman, E., & Ventura, D. (2006, July). Spatiotemporal pattern recognition via liquid state machines. In *Neural Networks, 2006. IJCNN'06. International Joint Conference on* (pp. 3848-3853). IEEE.
- [12] Norton, D., & Ventura, D. (2010). Improving liquid state machines through iterative refinement of the reservoir. *Neurocomputing*, 73(16-18), 2893-2904.
- [13] Maass, W., Legenstein, R. A., & Bertschinger, N. (2005). Methods for estimating the computational power and generalization capability of neural microcircuits. In *Advances in neural information processing systems* (pp. 865-872).
- [14] Nise, N. S. (2007). *CONTROL SYSTEMS ENGINEERING*, John Wiley & Sons.
- [15] Zhang, Y., Li, P., Jin, Y., & Choe, Y. (2015). A digital liquid state machine with biologically inspired learning and its application to speech recognition. *IEEE transactions on neural networks and learning systems*, 26(11), 2635-2649.
- [16] Smith, M. R., Hill, A. J., Carlson, K. D., Vineyard, C. M., Donaldson, J., Follett, D. R., ... & Aimone, J. B. (2017, May). A novel digital neuromorphic architecture efficiently facilitating complex synaptic response functions applied to liquid state machines. In *Neural Networks (IJCNN), 2017 International Joint Conference on* (pp. 2421-2428). IEEE.
- [17] Ju, H., Xu, J. X., Chong, E., & VanDongen, A. M. (2013). Effects of synaptic connectivity on liquid state machine performance. *Neural Networks*, 38, 39-51.
- [18] Buonomano, D. V., & Maass, W. (2009). State-dependent computations: spatiotemporal processing in cortical networks. *Nature Reviews Neuroscience*, 10(2), 113.
- [19] Slaney, M. (1998). *Auditory toolbox*. Interval Research Corporation, Tech. Rep, 10, 1998.
- [20] Schrauwen, B., & Van Campenhout, J. (2003, July). BSA, a fast and accurate spike train encoding scheme. In *Proceedings of the international joint conference on neural networks* (Vol. 4, No. 4, pp. 2825-2830). Piscataway, NJ: IEEE.
- [21] Lyon, R. (1982, May). A computational model of filtering, detection, and compression in the cochlea. In *Acoustics, Speech, and Signal Processing, IEEE International Conference on ICASSP'82. (Vol. 7, pp. 1282-1285). IEEE.*
- [22] Tavanaei, A., & Maida, A. S. (2017). A spiking network that learns to extract spike signatures from speech signals. *Neurocomputing*, 240, 191-199.
- [23] Dibazar, A. A., Song, D., Yamada, W., & Berger, T. W. (2004, July). Speech recognition based on fundamental functional principles of the brain. In *Neural Networks, 2004. Proceedings. 2004 IEEE International Joint Conference on* (Vol. 4, pp. 3071-3075). IEEE.
- [24] Wade, J. J., McDaid, L. J., Santos, J. A., & Sayers, H. M. (2010). SWAT: a spiking neural network training algorithm for classification problems. *IEEE Transactions on Neural Networks*, 21(11), 1817-1830.
- [25] Luo, S., Guan, H., Li, X., Xue, F., & Zhou, H. (2018, November). Improving liquid state machine in temporal pattern classification. In *2018 15th International Conference on Control, Automation, Robotics and Vision (ICARCV)* (pp. 88-91). IEEE.